Supplementary Information (SI) for Materials Horizons.
This journal is © The Royal Society of Chemistry 2025

Supplementary Materials for

Discovery of magnetic field line dependent anisotropic chemiresistive response in Magnetite: A new piece to the puzzle of magnetoreception

Pratyasha Rudra[a,b] and Swastik Mondal[*a,b]

[a]CSIR-Central Glass and Ceramic Research Institute; Jadavpur, Kolkata-700032, India

[b]Academy of Scientific and Innovative Research (AcSIR); Ghaziabad- 201002, India

*E-mail: swastik_mondal@cgcri.res.in

The PDF file includes:

1. Supplementary Discussion
2. Supplementary Figures (Figs. S1 to S13)
3. Supplementary Tables (Tables S1 to S9)

Supplementary Discussion

Rietveld refinement details

Magnetite crystal structure refinement was performed using the Rietveld method[63] with the Jana2006 program, following standard procedures.[25] The refinement employed the space group *Fd-3m* and a Pseudo-Voigt profile function for the magnetite sample. Background points were modeled using Legendre polynomials with 30 terms. The isotropic thermal parameter of the oxygen atom could not be refined freely alongside other parameters. To address this, a fixed isotropic thermal parameter for oxygen was used in the final refinement cycles. The final refinement cycle was conducted with damping factor 1. The excellent agreement between experimental and calculated XRD patterns (Fig. 1a), along with the reliability factor values (Table S9), confirms the accuracy of the crystal structure model.

Crystal and Microstructure

X-ray diffraction (XRD) data reveals that the magnetite exhibits a cubic structure with an Fd-3m (1) space group and a lattice parameter of 8.4049(5) Å. High-resolution transmission electron microscopy (HRTEM) and its corresponding fast Fourier transform (FFT) were used to identify the crystallographic planes. The crystallographic (113) plane has been found to be one of the most exposed planes in magnetite. Microstructural analysis using both TEM and Field Emission Scanning Electron Microscope (FESEM) demonstrates the formation of well-defined nano-spheres. Energy dispersive X-ray spectroscopy (EDX) confirms the presence of iron (Fe) and oxygen (O) in the sample.

Surface Electronic States

The surface electronic states of distinct elements (Fe, O), as well as surface oxygen vacancies, were investigated using X-ray photoelectron spectroscopy (XPS) using computer program KOIXPD. The background of the core-level spectra was modeled using the Shirley algorithm and the Fe 2p and O 1s core-level spectra were fitted using a least squares non-linear fitting method (Fig. 1(g)-(i)). In this process, the Fe 2p and O 1s core-level spectra were deconvoluted using a combination of Gaussian and Lorentzian profile functions.

The bivalence of iron is evident from Fig. 1(g)-(i) which confirms formation of magnetite. Additionally, the O 1s spectrum reveals a small amount of oxygen vacancies in the sample.

The ratio of the area under the curves of Fe^{2+} to Fe^{3+} has been found to be 0.42 after scaling with the photoionization cross-section values specific to the corresponding orbitals. This Fe^{2+}/Fe^{3+} ratio is probably likely due to charge balance on the surface because of the presence of oxygen vacancies.

Magnetoresistance

Hall measurement results yielded a Hall coefficient R_H value of -4.876×10^7 cm^3/C, indicating the presence of negative charge carriers. Additionally, the magnetoresistance of the magnetite pellet was found to be 3.45 MΩ, which closely aligns with the results observed in our sensing experiments using the magnetite thin-film sensor (~2-4 MΩ). Resistivity of magnetite and mobility of charge carriers have been found to be 6.71×10^5 Ωcm and 72.7 cm^2/Vs respectively.

Magneto-chemiresistance

As illustrated in Fig. S10, upon introducing a magnetic field using the bar magnet directed to geomagnetic north, there is an observed increase in the base resistance, indicating a positive total magnetoresistance (R^D_{TMR}) of magnetite under the magnetic field along direction D (Table S6).

$$R^D_{TMR} = R^D_{OMR}+R^D_{AMR}= (R^D_0 - R_0) \quad (S1)$$

Where, R_0 = Base resistance when H=0, R^D_0 = Base resistance of magnetite for a particular field direction, R^D_{OMR} = Ordinary magnetoresistance with field line along D, R^D_{AMR} = Anisotropic magnetoresistance due to field line along D.

And, then altering the direction of the field line relative to geomagnetic north manifests changes in base resistance in magnetite, indicating the involvement of change in anisotropic magnetoresistance (R^D_{AMR}) alongside change in ordinary magnetoresistance (R^D_{OMR}). So, these change in base resistance due to the change in field line direction has been denoted as,

$$\mathbf{\Delta}R^D_{TMR} =(\mathbf{\Delta}R^D_{OMR+AMR}) = (R^D_0 - R^N_0) \quad (S2)$$

Where, R^N_0 = Base resistance of magnetite when magnet field lines align towards north.

Then equation S3 delineates the concept of total magneto-chemiresistance (R^D_{TMCR}), denoting the final resistance of magnetite subsequent to purging it with analyte under a magnetic field along a particular direction. The observed change in resistance, indicating a negative shift in the magneto-chemiresistance of magnetite, is denoted as $\mathbf{\Delta}R^D_{MCR}$ (Fig. S3 to S6 and S10 and

Table S6 and S7). It has been observed that alterations in the field strength and field line direction alter the value of R^D_{TMCR} indicating the dependence of magneto-chemiresistance on the strength and direction of the magnetic field (Fig. S10 and Table S6). This pattern is observed consistently across all directions.

$$R^D_{TMCR} = R_0 + R^D_{TMR} + \mathbf{\Delta}R^D_{MCR} \quad \text{(S3)}$$

Where, is R^D_{TMCR} = Total magneto-chemiresistance with field lines directed along D, R^D_{TMR} = Total magnetoresistance experienced by the magnetite-based sensor with field line along D, $\mathbf{\Delta}R^D_{MCR}$ = Change in magneto-chemiresistance due to field line along D.

$$\mathbf{\Delta}R^D_{MCR} = \mathbf{\Delta}R^D_{OMCR} + \mathbf{\Delta}R^D_{AMCR} + \mathbf{\Delta}R_{CR} \quad \text{(S4)}$$

Where changes in ordinary and anisotropic magneto-chemiresistance due to field line along D have been denoted as $\mathbf{\Delta}R^D_{OMCR}$ and $\mathbf{\Delta}R^D_{AMCR}$ respectively and $\mathbf{\Delta}R_{CR}$ is the normal chemiresistance change due to analyte.

Changes in magneto-chemiresistance along with changes in magnetoresistance yield distinct magneto-chemiresistive response values along different directions (Table S6-S7).

Figures

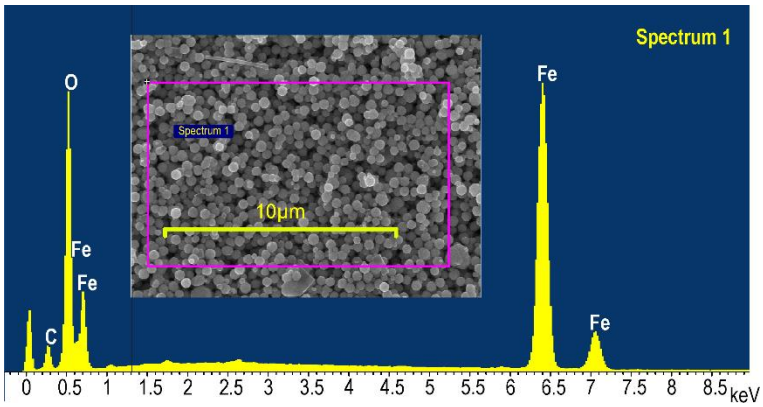

Fig. S1. EDX spectra of magnetite.

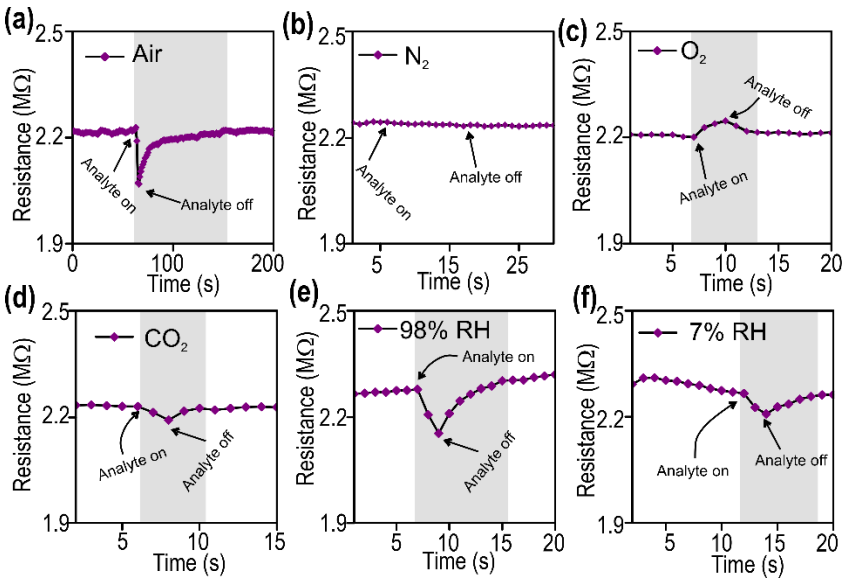

Fig. S2. Dynamic resistance change curve from chemiresistive sensing experiments using magnetite sensor. Dynamic resistance changes of magnetite upon purging (a) Air. (b) Pure nitrogen gas (99.99%). (c) 20% oxygen gas (Nitrogen balanced). (d) 0.04% carbon dioxide (Nitrogen balanced). (e) 98% relative humidity. (f) 7% relative humidity.

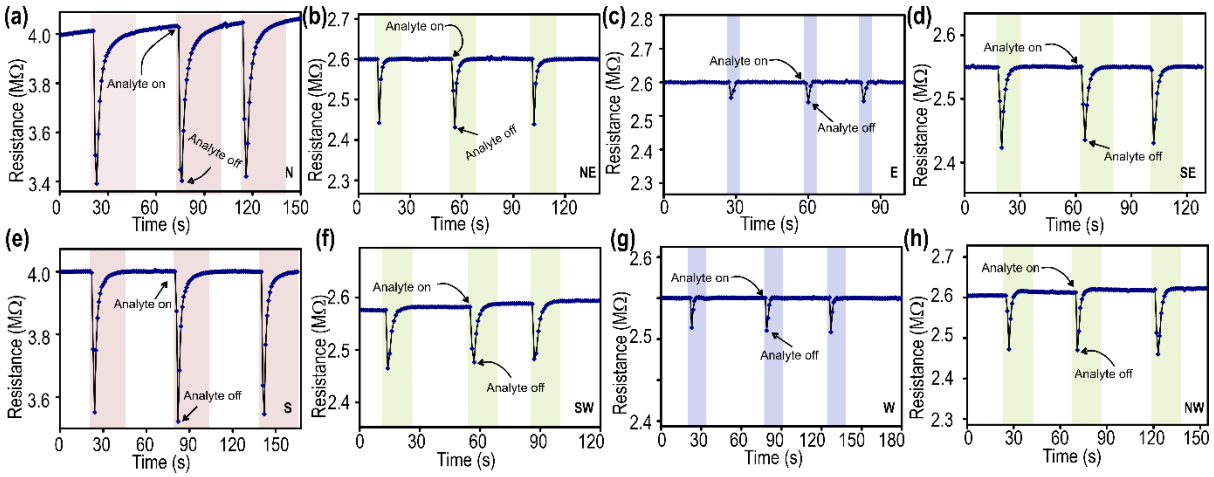

Fig. S3. Magneto-chemiresistive sensing of magnetite to 98% RH. (a) to (h) Dynamic resistance change curve of field line direction dependent magneto-chemiresistive sensing response for different directions (Direction indicated in each Fig. are denoted using conventional abbreviations).

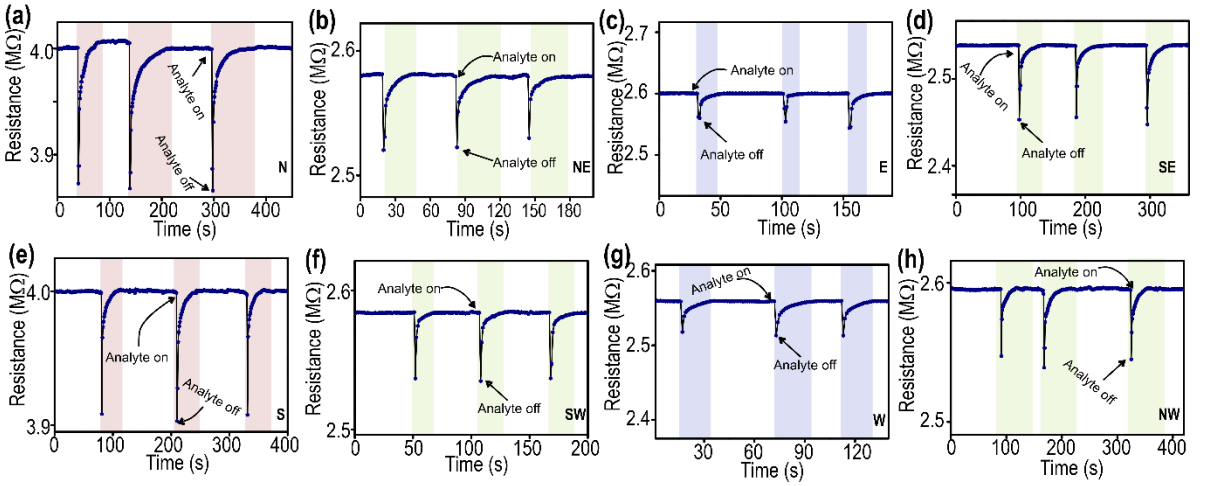

Fig. S4. Magneto-chemiresistive sensing of magnetite to 7% RH. (a) to (h) Dynamic resistance change curve of field line direction dependent magneto-chemiresistive sensing response for different directions (Direction indicated in each Fig. are denoted using conventional abbreviations).

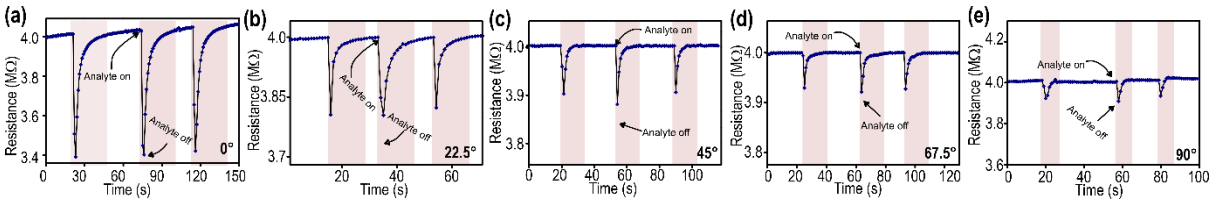

Fig. S5. Magneto-chemiresistive sensing of magnetite to 98% RH varying inclination angle of magnetite sensor. (a) to (e) Plots of dynamic resistance change of magnetite varying inclination angles while bar magnet was directed to geomagnetic north (Inclination angle of sensor is mentioned at right-bottom side of each plot).

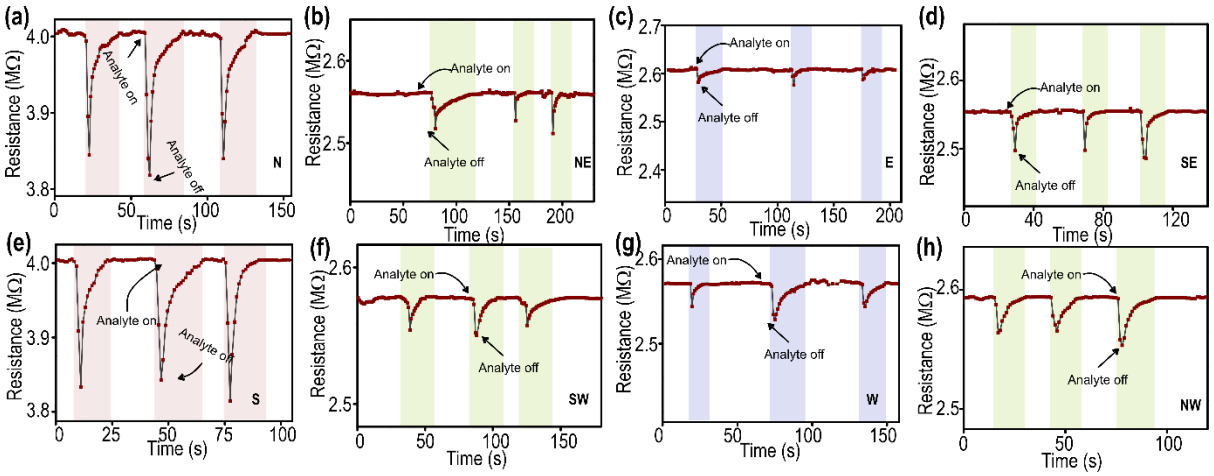

Fig. S6. Magneto-chemiresistive sensing of magnetite to 98% RH under white light. (a) to (h) Dynamic resistance change plots of field line direction dependent magneto-chemiresistive sensing response for different directions under white light (Directions are mentioned at right-bottom sides of each Fig. and denoted with conventional abbreviation).

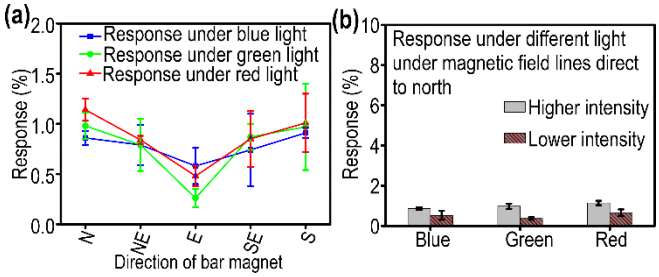

Fig. S7. Direction dependent magneto-chemiresistive response to 98% RH by magnetite under three primary colors of light. (a) Changes in magneto-chemiresistive response at different field line direction under blue, green, red light. (b) Changes in magneto-chemiresistive response under blue, green, red light, each with intensities 1800 and 3600 mcd, when field lines of bar magnet were aligned to geomagnetic north.

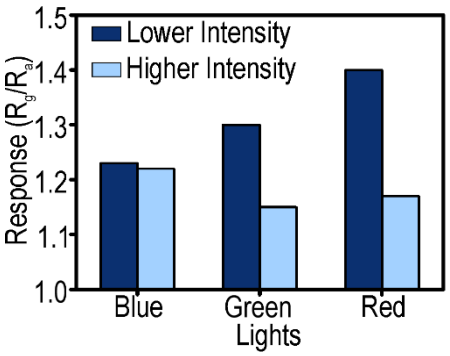

Fig. S8. Changes in magneto-chemiresistive response to 20 ppm NO_2 under blue, green, red light, each with intensities 1800 and 3600 mcd, when field lines of bar magnet were aligned to geomagnetic north.

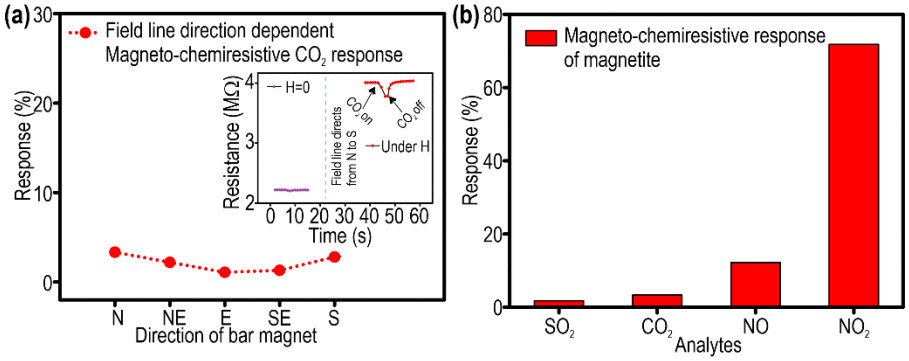

Fig. S9. Direction dependent magneto-chemiresistive response to CO_2 by magnetite and cross response of magnetite under magnetic field. Magneto-chemiresistive response for different directions of the bar magnet: (a) In presence of CO_2 (inset: dynamic resistance change without magnetic field and under magnetic field where response towards CO_2 has been found 3.33% while the magnetic field lines were directed to geomagnetic north) (b) Cross sensing response of magnetite to different toxic analytes where, in presence of NO_2 highest response has been found 71.80% while the magnetic field lines were directed to geomagnetic north.

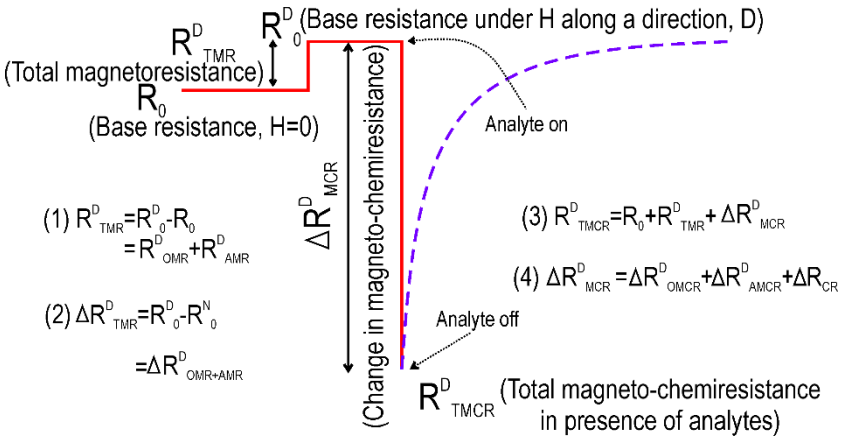

Fig. S10. Schematic diagram of magneto-chemiresistive resistance and its components. In magneto-chemiresistive response formula, R_0 = Base resistance when H=0, R^D_0 = Base resistance of magnetite in a particular direction of field, R^D_{OMR} = Ordinary magnetoresistance with field line along D, R^D_{AMR} = Anisotropic magnetoresistance due to field line along D, R^N_0 = Base resistance of magnetite when magnet field lines align towards north, R^D_{TMCR} = Total magneto-chemiresistance in a particular direction, R^D_{TMR} = Total magnetoresistance experienced by the magnetite-based sensor with field line along D, ΔR^D_{MCR} = Changes in magneto-chemiresistance due to field line along D, ΔR^D_{OMCR} and ΔR^D_{AMCR} are changes in

ordinary and anisotropic magneto-chemiresistance respectively due to field line along D and ΔR_{CR} is the normal chemiresistance change due to analyte.

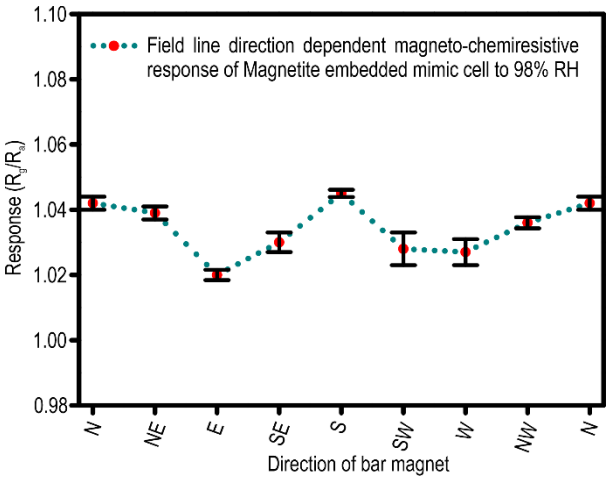

Fig. S11. Direction-dependent magneto-chemiresistive response to 98% RH by magnetite embedded in hydrogel.

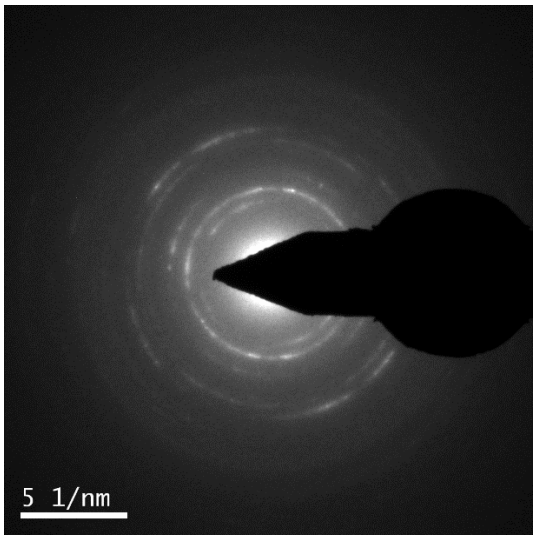

Fig. S12. SAED pattern of poly crystalline Magnetite showing ring pattern.

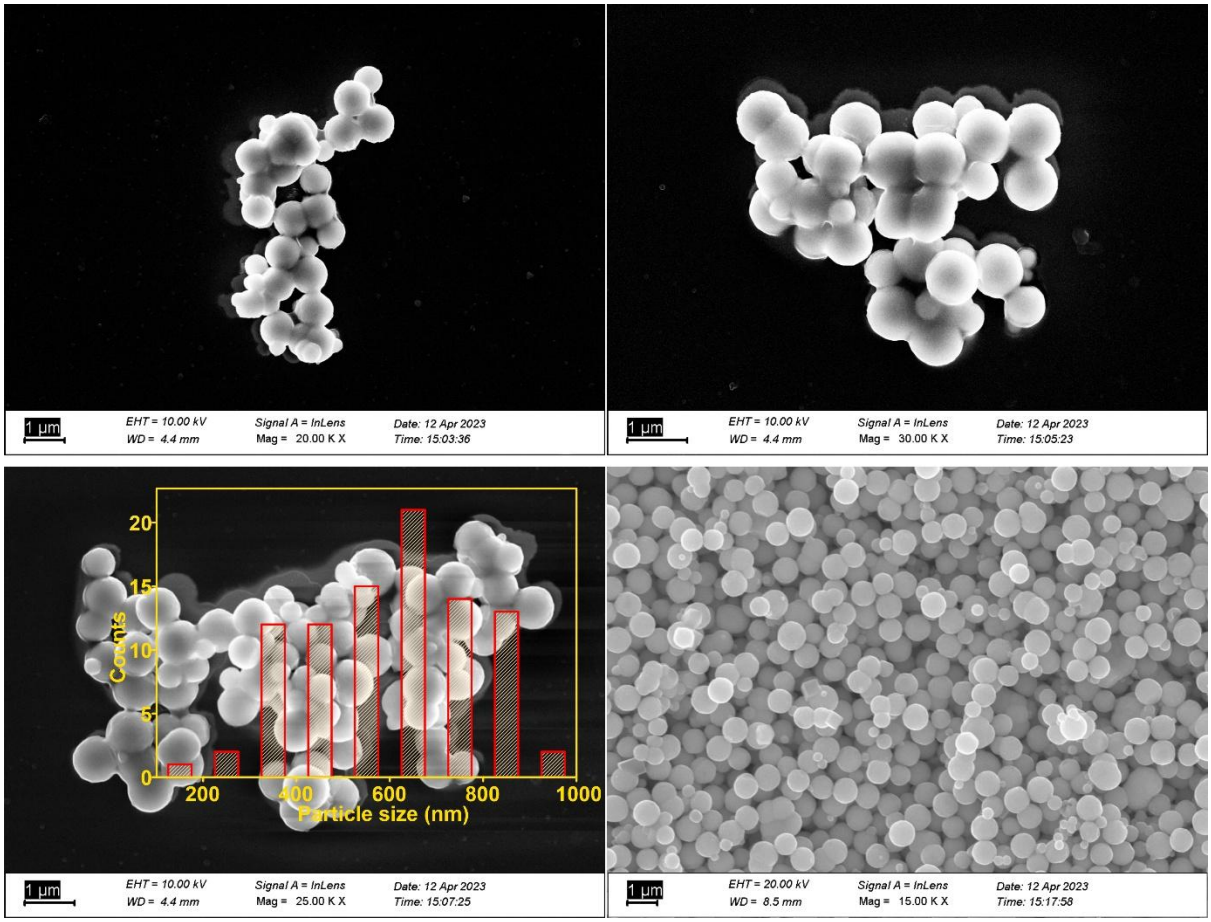

Fig. S13. FESEM images at different magnifications, along with a particle size distribution histogram.

Tables

Table S1: Chemiresistive response of magnetite towards various analytes

Analyte	Chemiresistive response value (%/times)
Air	1.70(4)
N_2	0
CO_2	0.33(5)
98% RH	0.58(2)
7% RH	0.48(2)
NO_2	1.028(1) (in times)
O_2	1.013(1) (in times)

Table S2: Magneto-chemiresistive response of magnetite towards 98% RH under different magnetic field strength

Magnetic Field (mT)	Response (%)
0.02	9.40(6)
0.05	15.33(26)
1.13	31.33(91)
2.6	3.74(8)
3.21	2.07(8)

Table S3: Field line direction and inclination angle dependent magneto-chemiresistive response of magnetite sensor

Direction of bar magnet (geomagnetic directions)	Direction dependent Magneto-chemiresistive response (%)		Inclination angle dependent magneto-chemiresistive sensing	
	Without light	Under white light	Inclination angle of sensor (°)	Response (%)
North	15.33(26)	4.05(39)	0	15.33(26)
North East	5.68(13)	1.51(22)	22.5	6.65(22)
East	1.25(2)	0.62(14)	45	2.95(22)
South East	4.95(16)	1.66(12)	67.5	2.31(8)
South	12.51(25)	3.96(85)	90	1.86(22)
South West	4.71(9)	1.16(8)	-	-
West	2.21(27)	0.72(12)	-	-
North West	4.79(64)	1.42(16)	-	-

Table S4: Magnetic field line direction dependent magneto-chemiresistive response to 7% RH

Direction of bar magnet (geomagnetic directions)	Magneto-chemiresistive response (%) to 7% RH
North	2.87(3)
North East	1.70(4)
East	1.20(15)
South East	1.74(12)
South	2.24(5)
South West	1.47(5)
West	1.30(9)
North West	1.64(4)

Table S5: Magnetic field line direction dependent magneto-chemiresistive response to 98% RH under different light illuminations

Direction of bar magnet (geomagnetic directions)	Response (%)		
	Blue light	Green light	Red light
North	0.86(7)	0.98(13)	1.14(11)
North East	0.79(20)	0.79(26)	0.84(4)
East	0.58(18)	0.26(9)	0.48(10)
South East	0.74(36)	0.87(13)	0.85(28)
South	0.91(5)	0.97(43)	1.01(29)
West	0.41(20)	0.37(6)	0.51(10)

Table S6: Magneto-chemiresistance and its components

Direction of bar magnet (geomagnetic directions)	$R^D_{TMCR} = [(R_0 + R^D_{TMR}) + \Delta R^D_{MCR}] = [R^D_0 + \Delta R^D_{MCR}]$ (MΩ)			
	R_0 (MΩ)	R^D_0 (MΩ)	R^D_{TMCR} (MΩ)	ΔR^D_{MCR} (MΩ)
Without Magnetic field	2.228(21)	-	-	-
North	-	4.031(11)	3.413(19)	-0.618(22)
South	-	4.031(24)	3.526(23)	-0.504(33)
East	-	2.613(8)	2.580(8)	-0.033(11)
West	-	2.563(1)	2.513(6)	-0.050(6)
North East	-	2.569(13)	2.423(13)	-0.146(19)
South West	-	2.585(1)	2.464(4)	-0.122(4)
North West	-	2.594(2)	2.470(2)	-0.124(15)
South East	-	2.532(9)	2.397(12)	-0.125(15)

Table S7: Magneto-chemiresistance and its components

Direction of bar magnet (geomagnetic directions)	$\sum_{i=1}^{n}[R^{D}_{TMR}]_i$ (MΩ) [where, $R^{D}_{TMCR} = R_0 + R^{D}_{TMR} + \Delta R^{D}_{MCR}$]	Chemiresistive detection value of magnetite towards 98% RH	Magneto-chemiresistive detection value of magnetite towards 98% RH	Change in magneto-resistance (Ordinary + Anisotropic) due to change of bar magnet direction (MΩ)
		$\sum_{i=1}^{n}[\ [R_g\text{-}R_a/R_a]_i$	$\sum_{i=1}^{n}[\ \lvert(\Delta R^{D}_{MCR})\rvert\ /\ R^{D}_{0}]_i$	$\Delta R^{D}_{OMR+AMR}=\sum_{i=1}^{n}[R^{D}_{0}\text{-}R^{N}_{0}]_i$ (MΩ)
Without Magnetic field	-	0.58(2)	-	-
North	1.803(11)	-	0.1533(26)	0
South	1.803(4)	-	0.1251(25)	-0.001(12)
East	0.385(14)	-	0.0125(2)	-1.419(3)
West	0.342(20)	-	0.0221(27)	-1.461(10)
North East	0.341(13)	-	0.0568(13)	-1.463(5)
South West	0.357(20)	-	0.0471(9)	-1.446(10)
North West	0.367(20)	-	0.0479(64)	-1.437(9)
South East	0.304(12)	-	0.0495(16)	-1.500(3)

Table S8: The AMR ratio reported in previous studies on various Fe-based oxides.

Temperature (K)	AMR ratio formula	AMR ratio	Magnetic field	Reference
300	$(\Delta\rho/\rho_0)\%$	<0.2	-	52
293	$(\Delta\rho/\rho_0)\%$	1.2	23.4 mT	55
293	$(\Delta\rho/\rho_0)\%$	1.7	22.8 mT	55
180	$(\Delta\rho/\rho_0)\%$	0.5±0.02	1 T	56
75-125	$(\Delta\rho/\rho_0)\%$	~0.75	-	57
300K	$(\Delta\rho/\rho_0)\%$	0-0.35	5 T	58
70K	$(\Delta\rho/\rho_0)\%$	0-(-1.5)	0.5-50 kOe	59
150K	$(\Delta\rho/\rho_0)\%$	0.9965-1	9T	60
298	$\Delta R/R_0$	0.54	0.05 mT	This work

Table S9: Rietveld refinement results and crystal structure parameters

R_p/wR_p/GOF	4.61/6.47/1.29
a=b=c in Å	8.4049(2)
V (Å^3)	593.74(1)
Fe1: x=y=z	0.625
Fe2: x=y=z	0
O: x=y=z	0.3767(2)
Fe1-O (Å)	2.08(2)
Fe2-O (Å)	1.8445(19)
U_{iso}: Fe1/Fe2/O	0.0038(3)/0.0109(5)/0.025